Nonlinear Processes in Geophysics (1995) 2: 280 - 289

Nonlinear Processes in Geophysics

Asymmetry of wind waves studied in a laboratory tank

I. A. Leykin[1], M. A. Donelan[2], R. H. Mellen[3] and D. J. McLaughlin[1]

[1] Northeastern University, Boston, MA 02115, USA
[2] National Water Research Institute, Canada Centre for Inland Waters, Burlington, Ontario L7R 4A6, Canada
[3] Marine Sciences Institute, The University of Connecticut, Groton, Connecticut 06340, USA

Received 21 April 1995 - Accepted 22 June 1995 - Communicated by V. Shrira

Abstract. Asymmetry of wind waves was studied in a laboratory tank under varied wind and fetch conditions using both bispectral analysis of wave records and third-order statistics of the surface elevation. It is found that skewness S (the normalized third-order moment of the surface elevation describing the horizontal asymmetry of waves) varies only slightly with the inverse wave age u_*/C_m (where u_* is the air friction velocity and C_m is the phase speed of the dominant waves). At the same time asymmetry A, which is determined from the Hilbert transform of the wave record and characterizes the skewness of the rate of change of surface elevation, increases consistently in magnitude with the ratio u_*/C_m. This suggests that nonlinear distortion of the wave profile is determined by the degree of wind forcing and is a sensitive indicator of wind-wave interaction processes.

It is shown that the asymmetric profile of waves can be described within the frameworks of the nonlinear nonspectral concept (Plate, 1972; Lake and Yuen, 1978) according to which the wind-wave field can be represented as a coherent bound-wave system consisting mainly of the dominant component ω_m and its harmonics propagating with the same speed C_m, as observed by Ramamonjiarisoa and Coantic (1976). The phase shift between ω_m and harmonics is found and shown to increase with the asymmetry of the waves.

1 Introduction

Asymmetry of wind waves (wave crests are sharpened and tilted forward) is a well-known feature of the roughened sea surface that leads to non-Gaussianity of the surface statistics and is of considerable interest for interpreting microwave backscattering from the sea, parametrization of wave breaking processes, and modeling the air flow over surface waves. A few attempts have been made to investigate asymmetry of waves using the third-order statistics of the surface elevation (Huang and Long, 1980) or slopes (Longuet-Higgins, 1982) as well as the "individual wave" approach (Bailey et al., 1991), yet the detailed description of the distorted wave form and its dependence on wave-generation conditions is still insufficiently studied.

On the other hand, asymmetry of the wave profile indicates the importance of nonlinear effects in the surface geometry and therefore is intimately bound to the problem of nonlinear coupling within the wave spectrum. Thus, asymmetry of waves can not be described within the framework of the conventional linear spectral model that represents the roughened sea surface as a superposition of spectral components with random phases (Phillips, 1977). Alternative approaches to a description of the random wave field were proposed by Plate (1972), Ramamonjiarisoa and Coantic (1976), and Lake and Yuen (1978). According to their concept, which will be hereinafter refered to as the nonlinear nonspectral concept, wind waves are treated as a coherent bound-wave system consisting mainly of the dominant component ω_m and its harmonics propagating with the same speed.

In the general case both free and bound waves are present in a wind-wave spectrum, and the predominance of one over the other depends on the degree of wind forcing (Donelan et al., 1985). However, the actual structure of the wind-wave spectrum that leads to the asymmetric wave form is still very poorly understood.

Bispectral analysis (Nikias and Raghuveer, 1987) is a useful tool for this purpose. As applied to wind waves, bispectral analysis was introduced by Hasselmann et al. (1963) and later applied to both field and laboratory data (e.g., Imasato and Kunishi, 1977; Masuda and Kuo, 1981; Yefimov and Kalmykov, 1984). The clearest application of the bispectral technique to surface waves was fulfilled by Elgar and Guza (1985) who studied substantially nonlinear

Correspondence to: I. A. Leykin

waves in the shallow near-shore zone and demonstrated the relationship between bispectral properties of waves and asymmetry of the wave form. However, no such data are available now for deep-water wind waves.

The purpose of this paper is to study asymmetric wave forms of wind waves measured in a laboratory tank using both third-order surface statistics and bispectral analysis. Basic definitions of the bispectral technique as applied to analysis of asymmetric wave records are summarized in §2. The procedure of wave measurements and data analysis is described in §3, and results of the measurements are presented in §4. In §5 our experimental results are discussed and conclusions are made.

2 Bispectral Analysis of Asymmetric Wave Records

The asymmetric properties of a wave record corresponding to a random process $\zeta(t)$ can be described by its normalized third-order moments, hereinafter called skewness S and asymmetry A. Skewness indicates asymmetry of the wave form with respect to the horizontal axis and is determined directly from the record

$$S = <\zeta^3> / \sigma^3 \tag{2.1}$$

where $\sigma = (<\sigma^3>)^{1/2}$ and $<...>$ represents statistical averaging. Asymmetry A measures asymmetry of the wave form with respect to the vertical axis and is determined from the Hilbert transform of the process $\zeta_H(t)$ (Elgar, 1987)

$$A = <\zeta_H(t)^3> / \sigma^3 \tag{2.2}$$

Note that as applied to the record of water waves, it is commonly assumed that the horizontal axis x corresponds to the stable water surface and that the surface elevation z is measured along the vertical axis z.

The complex bispectrum $Bi(\omega_1, \omega_2)$, or the third-order spectrum, can be determined directly from the complex Fourier coefficients of the process $F(\omega_n)$:

$$Bi(\omega_1, \omega_2) = <F(\omega_1) F(\omega_2) F^*(\omega_1+\omega_2)> \tag{2.3}$$

where

$$F(\omega_n) = |F(\omega_n)| \exp(-i\phi_n) \tag{2.4}$$

$\omega=2\pi f$ is the radian frequency; $\phi_n= \omega_n t + \psi_n$ is a phase; and an asterisk * indicates complex conjugation. The bispectrum (2.3) is symmetrical with respect to the diagonal $\omega_1=\omega_2$, and its real and imaginary parts are related, respectively, to skewness S and asymmetry A (see Elgar, 1987).

The bispectrum (2.3) indicates a degree of three-wave coupling between wave components

$$\omega_1 + \omega_2 \rightarrow \omega_3 = (\omega_1 + \omega_2) \tag{2.5}$$

If the process is linear, the Fourier coefficients $F(\omega_n)$ have random phases ϕ_n and the bispectrum is zero. However, if the process has an asymmetric wave form, at least some of its Fourier components $F(\omega_n)$ have a non-random relationship between their phases which leads to a non-zero bispectrum. Consequently, the bispectrum provides important information on the nonlinear coupling within the wave spectrum.

The bicoherence (normalized magnitude of the bispectrum) and biphase are commonly defined as follows (Kim and Powers, 1979)

$$b^2(\omega_1, \omega_2) = |Bi(\omega_1, \omega_2)|^2 / [G(\omega_1, \omega_2) E(\omega_1 + \omega_2)] \tag{2.6}$$

$$\beta(\omega_1, \omega_2) = \arctan\{Im[Bi(\omega_1, \omega_2)] / Rc[Bi(\omega_1, \omega_2)]\} \tag{2.7}$$

where

$$E(\omega_1+\omega_2) = <|F(\omega_1, \omega_2)|^2> \tag{2.8}$$

$$G(\omega_1, \omega_2) = <|F(\omega_1) F(\omega_2)|^2> \tag{2.9}$$

Biphase can be also represented in terms of the phases of the spectral components ω_1, ω_2, and $\omega_3= \omega_1+\omega_2$

$$\beta(\omega_1, \omega_2) = \phi_1 + \phi_2 - \phi_3 \tag{2.10}$$

In the general case of a broad-band process where any particular component can be involved in many interactions, the bicoherence (2.6) indicates a relative degree of phase coupling between wave triads, with $b^2=0$ for random phase relationship and $b^2=1$ for a maximum coupling; however, no simple interpretation of the bispectral data is possible (McComas and Briscoe, 1980).

Consider a special case of a narrow-band nonlinear process consisting of the dominant component ω_m and its harmonics

$$\zeta(t) = a_m [\cos\phi_1 + a_2\cos(2\phi_m + \Delta\phi_2) + a_3\cos(3\phi_m + \Delta\phi_3) + a_4\cos(3\phi_m + \Delta\phi_4) + ...] + \eta(t) \tag{2.11}$$

where $\phi_m= \omega_m t + \psi$ is the phase of the dominant component and a_m is its magnitude; a_i is the relative

magnitude of the i-th harmonic; $\Delta\phi_i$ is the phase shift of the harmonic with respect to the dominant component; $\eta(t)$ is random noise. The process (2.11) can be represented in terms of a three-wave interaction scheme known as a quadratic phase coupling (Nikias and Raghuveer, 1987) and describes a specific relationship between the frequencies and phases of three spectral components ω_1, ω_2, and ω_3 when $\omega_3 = \omega_1 + \omega_2$ and $\phi_3 = \phi_1 + \phi_2 + \Delta\phi$ (where $\Delta\phi$ is a non-random phase shift):

$$\omega_m+\omega_m \rightarrow 2\omega_m; \qquad \omega_m+2\omega_m \rightarrow 3\omega_m;$$

$$\omega_m+3\omega_m \rightarrow 4\omega_m; \qquad \ldots \qquad (2.12)$$

From (2.10-2.12) it follows that

$$\beta(\omega_m, \omega_m) = -\Delta\phi_2; \quad \beta(\omega_m, 2\omega_m) = \Delta\phi_2 - \Delta\phi_3;$$

$$\beta(\omega_m, 3\omega_m) = \Delta\phi_3 - \Delta\phi_4; \quad \ldots \qquad (2.13)$$

Consequently, phase shifts $\Delta\phi_i$ that appear in (2.11) can be estimated from the biphase data

$$\Delta\phi_2 = -\beta(\omega_m, \omega_m);$$

$$\Delta\phi_3 = -[\beta(\omega_m, \omega_m) + \beta(\omega_m, 2\omega_m)];$$

$$\Delta\phi_4 = -[\beta(\omega_m, \omega_m) + \beta(\omega_m, 2\omega_m) + \beta(\omega_m, 3\omega_m)];$$

$$\ldots \qquad (2.14)$$

Note that the fourth harmonic $4\omega_m$ can be represented also as $2\omega_m + 2\omega_m \rightarrow 4\omega_m$. However, the bispectral estimate $Bi(2\omega_m, 2\omega_m)$ corresponding to this representation, is separated in the two-dimensional frequency domain (ω_1, ω_2) from the main estimate $Bi(\omega_m, 2\omega_m)$, so that the phase shift $\Delta\phi_4$ can be unambiguously determined from (2.14).

The representation (2.11) can be considered as a formal description of the nonlinear nonspectral concept. As will be shown below, this representation can be applied, though with some restrictions, to wind-wave records measured in a laboratory tank and used to investigate asymmetry of waves.

3 Wave Measurements and Data Analysis

The experiments were carried out at the Canada Centre for Inland Waters in a wind-wave tank that is 32.2 m long and 76 cm wide; the water depth was 22 cm and the wind tunnel was 63 cm high. Capacitance-type wave gauges were used to measure the surface elevation $\zeta(t)$ at five stations along the channel (fetch F from 4.2 to 28.6 m). Measurements were made for five centre-line wind speeds V=7.0, 10.5, 14.0, 17.5, and 21.0 m/s; the corresponding air friction velocities were, respectively, 0.27, 0.50, 0.82, 1.22, and 1.71 m/s. The air friction velocity u_* was not measured in this study but estimated from the calibration curves $u_* = u_*(V)$ available from previous measurements. Details of the facility are reported elsewhere (Ocampo-Torres et al., 1994).

The wave records $\zeta(t)$ of length from 500 to 675 sec. were digitized at a sampling rate of 40 Hz and processed to estimate the r.m.s. wave height $\sigma=(<\zeta^2>)^{1/2}$, skewness S, and asymmetry A. For bispectral analysis the wave record was divided into consecutive segments of 3.2 sec. each, the Fourier coefficients $F(\omega)$ were estimated for every segment using the FFT, and the bispectrum $Bi(\omega_1, \omega_2)$ was calculated with a frequency resolution of 0.312 Hz. Statistical averaging was performed over 100 segments to yield bispectral estimates with degrees of freedom d.o.f. $\approx$ 200.

According to Haubrich (1965), the 95% significance level of zero bicoherence is $b_o^2 \geq 6/\text{d.o.f.}$, which gives for our data $b_o^2 \approx 0.03$. The variance of the biphase depends on the corresponding values of the bicoherence b^2 (Elgar and Sebert, 1989) and is (in radians)

$$\text{Var}(\beta) = (1/\text{d.o.f.}) \; [(1/b^2) - 1] \qquad (3.1)$$

The power spectra $E(\omega)$ estimated with a frequency resolution of 0.156 Hz were used to determine the spectral maximum frequency ω_m which, in turn, was used to calculate the wavenumber of the dominant waves k_m. In the latter procedure one has to take into account the effect of the wind drift current on the phase velocity of waves C(k) (Stewart and Joy, 1974; Goncharov and Leykin, 1984; Shrira, 1993)

$$C(k) = C_o(k) + u_{av} \qquad (3.2)$$

where $C_o(k)$ is the phase velocity of surface waves in still water, u_{av} is some "averaged" value of the current appropriate to the wavenumber

$$u_{av}(k) = 2k \int_{0}^{-\infty} u(z) \exp(2kz) dz \qquad (3.3)$$

u(z) is the current's vertical profile, z is the depth. For a logarithmic drift profile (3.3) yields:

$$u_{av}(k) = u(z = -[1/(3.4\,k)]) \qquad (3.4)$$

Using Wu's (1975) estimate of the drift velocity at the

surface $u_s = 0.55u_*$ and assuming that the velocity profile in the upper half of the water column is logarithmic and determined by the stress on the surface, we have:

$$u(z) = u_* [\, 0.55 - (\rho_r^{1/2} / \kappa) \ln(-z / z_o) \,] \qquad (3.5)$$

where $\rho_r = 1.25 \cdot 10^{-3}$ is the ratio of air density to water density, and $k = 0.4$ is von Karman's constant. A detail analysis of the drift current in a laboratory tank (Ocampo-Torres et al., 1995) showed that under the conditions of our study, the current profile u(z) can be satisfactorily described choosing $z_o = 0.022$ cm which yields $u(z) \approx 0$ at mid depth. From (3.4) and (3.5) follows

$$u_{av}(k) = u_* [0.55 - (\rho_r^{1/2} / \kappa) \ln (1/(3.4\, kz_o))] \qquad (3.6)$$

Taking the finite water depth H into account, the dispersion relationship for surface waves in a current is

$$\omega = [\, gk \cdot \tanh(kH) + u_* [0.55 - (\rho_r^{1/2} / \kappa) \ln (1/ (3.4\, kz_o))\,] \qquad (3.7)$$

where g is the acceleration due to gravity. Eq.(3.7) was used to determine the wave number k_m from ω_m. After this, we estimated steepness of waves (or the mean wave slope) $\varepsilon_m = \sigma k_m$, the phase speed of the dominant waves $C_m = \omega_m / k_m$, and the ratio u_*/C_m (the inverse wave age).

4 Experimental Results

4.1 Parameters of Dominant Waves

As the wave field is developing under the action of the wind, waves' parameters vary significantly with both fetch and wind speed: from short gravity waves with r.m.s. wave height $\sigma \approx 0.5$-1.0 cm, spectral maximum frequency $f_m = \omega_m / 2\pi \approx 3.5$ Hz, and wave length $\lambda_m = 2\pi / k_m \approx 20$-$40$ cm observed at small fetch and low winds to longer and higher waves with $\sigma \approx 3.0$-3.5 cm, $f_m \approx 1.1$ Hz, and $\lambda_m \approx 120$-140 cm (large fetch and high winds).

For longer waves the effect of the finite water depth H=22 cm becomes important. If variation of the phase speed of waves C(k) is used as a criterion, then this effect is negligibly small under most conditions of our measurements. The effect of the finite depth on nonlinear distortion of the wave profile is more difficult to estimate; however, we found that in our measurements this effect manifests itself only at the largest fetch and under the highest wind speeds when $\lambda_m \geq 120$ cm. In this study, only the cases with $\lambda_m \leq 4H = 88$ cm were chosen, and we will assume that these data correspond to "deep-water" conditions.

Table 1. Spectral parameters of wind waves

No.	u_* [m/s]	F [m]	f_m [Hz]	σ [cm]	λ_m [cm]	u_*/C_m	ε_m	S	A
1	0.27	8.75	2.89	0.61	22.4	0.42	0.170	0.292	0.063
2	0.27	13.30	2.42	0.85	30.6	0.36	0.175	0.357	0.036
3	0.27	20.90	1.95	1.08	44.9	0.31	0.151	0.386	0.022
4	0.50	8.75	2.34	1.05	35.3	0.60	0.189	0.445	0.120
5	0.50	13.30	1.95	1.45	47.8	0.54	0.191	0.417	0.098
6	0.50	20.90	1.56	1.82	68.6	0.47	0.167	0.476	0.066
7	0.82	4.20	2.66	0.82	32.0	0.96	0.161	0.658	0.245
8	0.82	8.75	1.85	1.56	55.7	0.80	0.176	0.516	0.182
9	0.82	13.30	1.56	1.98	72.8	0.73	0.173	0.502	0.225
10	1.22	4.20	2.42	0.94	40.8	1.24	0.145	0.570	0.378
11	1.22	8.75	1.80	1.76	62.0	1.09	0.178	0.549	0.283
12	1.22	13.30	1.48	2.13	81.5	1.01	0.164	0.501	0.324
13	1.71	4.20	2.42	0.94	44.9	1.57	0.131	0.448	0.398
14	1.71	8.75	1.80	1.61	66.3	1.43	0.152	0.535	0.385
15	1.71	13.30	1.48	2.00	85.4	1.35	0.147	0.526	0.350

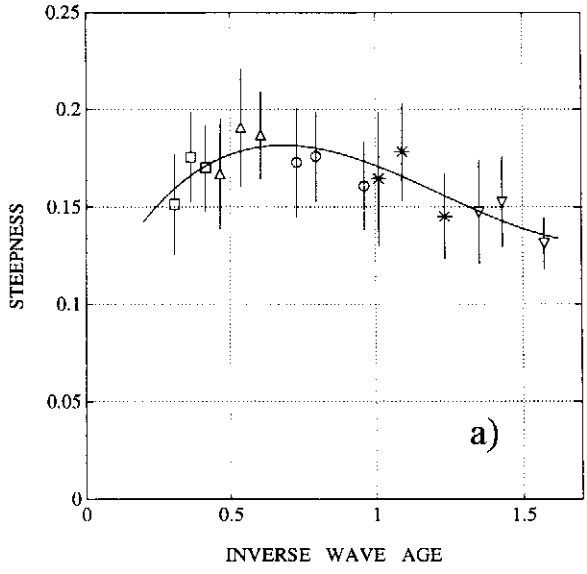

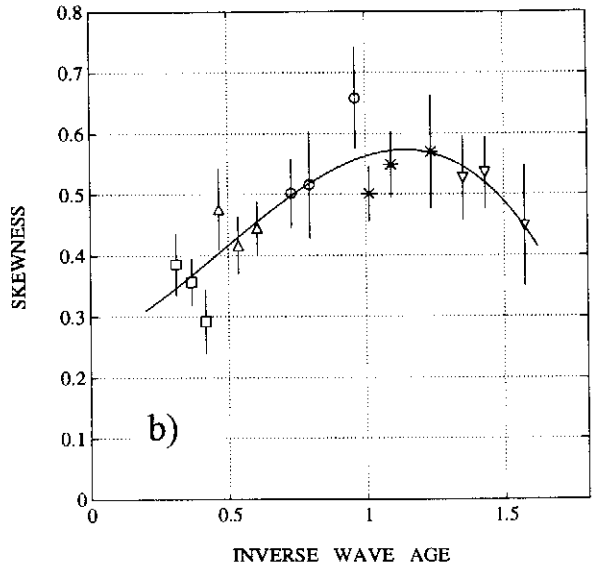

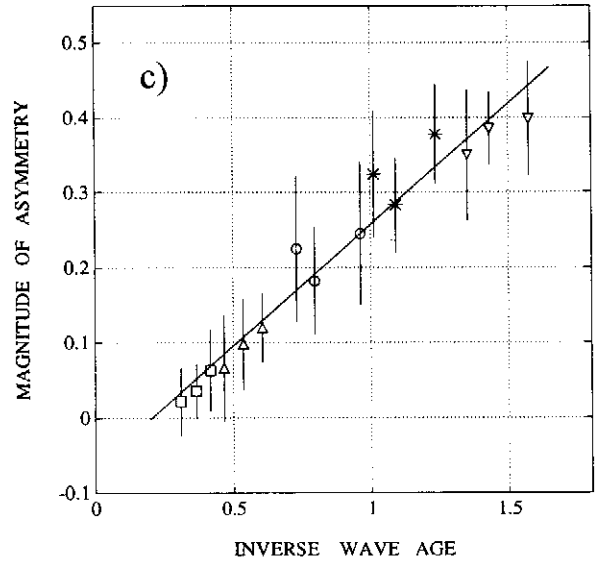

Fig.1. Variation of the steepness ε_m (a), skewness S (b), and magnitude of asymmetry -A (c) with inverse wave age u_*/C_m for different wind speeds u_*= 0.27 (□), 0.50 (Δ), 0.82 (○), 1.22 (*), and 1.71 m/s (▽). Solid lines in Fig.1a,b show an average trend of the data; a solid line in Fig.1c is the fit curve (4.1). Vertical bars are the standard errors.

In two cases (measurements at fetch F = 4.2 m for wind speeds u_*= 0.27m/s and 0.50m/s), the spectral maximum frequency $f_m \geq 3.5$ Hz was too high and the properties of harmonics could not be fully studied due to restrictions of our measuring procedure; these cases were excluded from further analysis. As a result, fifteen wave records were finally selected. Parameters of dominant waves for these records are given in Table 1.

The variation of the steepness ε_m, skewness S, and asymmetry A with inverse wave age u_*/C_m is shown in Fig.1. The steepness ε_m varies by less than ±15% about the mean value $\varepsilon_m \approx 0.165$. The skewness S reveals a more pronounced variation with u_*/C_m and is first increasing and then slightly decreasing. However, of most interest is the asymmetry A which increases systematically in magnitude (from 0 at $u_*/C_m \approx 0.3$ to -0.4 at $u_*/C_m \approx 1.2$). A negative sign of the asymmetry observed for all our data indicates that wave crests are tilted forward. A linear fit curve through the data shown in Fig.1c is

$$-A = -0.066 + 0.323 \cdot (u_*/C_m) \qquad (4.1)$$

4.2 Bispectral Properties of Wind Waves

Consider in detail the bispectral properties of one wave record (u_* = 1.22 m/s, fetch 4.20 m) that is typical of our measurements. The power spectrum of this record (Fig.2a) reveals a major peak at $f_m \approx 2.4$ Hz (the dominant component) and additional peaks at $f \approx 2f_m = 4.8$ Hz (the second harmonic) and at $f \approx 3f_m = 7.2$ Hz (the third harmonic). Such a spectral shape is commonly observed in laboratory tanks (e.g., Leykin et al., 1984).

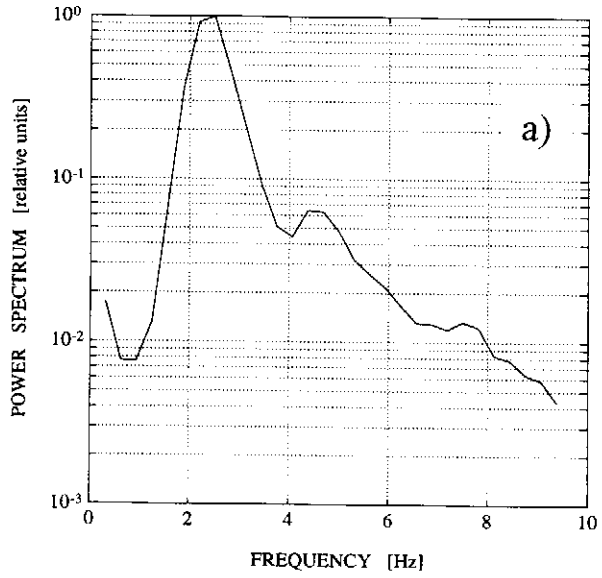

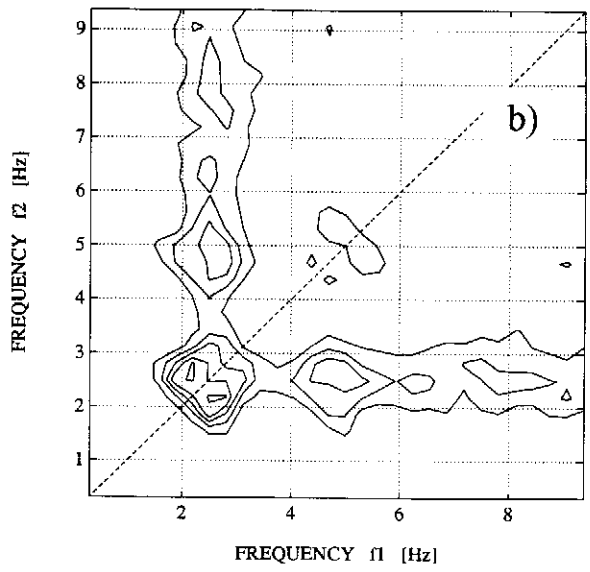

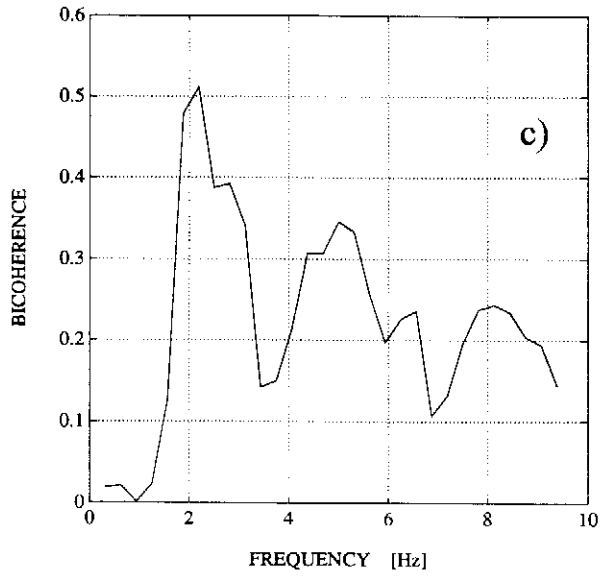

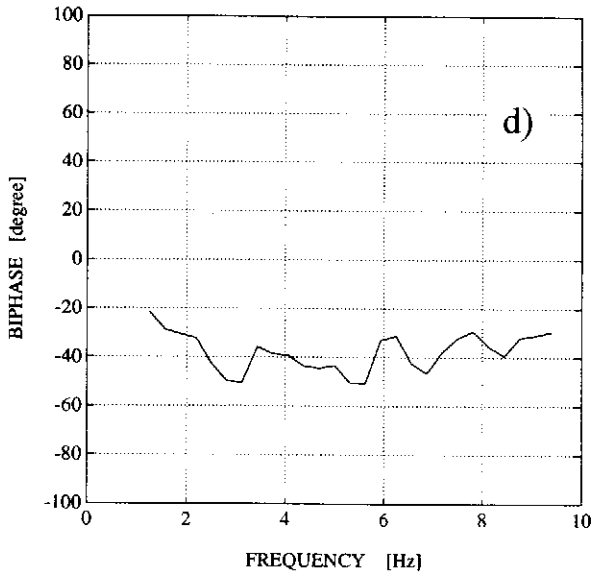

Fig.2. Bispectral properties of wind waves for a typical wave record (wind speed $u_* \sim 1.22$ m/s, fetch $F = 4.2$ m). (a) The power spectrum E(f) in relative units E(f) / E(f_m). (b) Contours of the bicoherence b^2 (f_1, f_2); the minimum contour level is 0.1 with additional contours every 0.1. (c,d) Cross-section of the bicoherence b^2 and biphase β at $f_1 = f_m$. The 95% significance level for the bicoherence is 0.03.

The bicoherence plot (Fig.2b) shows that a high bicoherence is concentrated mainly along the ridge $f \approx f_m$. A one-dimensional cross-section of the bicoherence and biphase for f_1=2.4 Hz (i.e., along this ridge) is shown in Fig.2c,d. The observed pattern of the bicoherence indicates that nonlinear interaction within the wave spectrum is mainly a coupling between the dominant component f_m and its harmonics. If so, one can perform a simple interpretation of the bispectral data using the representation (2.11) and estimate the phase shift of harmonics with respect to the dominant component f_m from (2.14).

Thus, a major peak in the bicoherence spectrum seen at $f \approx f_m = 2.4$ Hz with $b^2 = 0.5$ (Fig.2c) can be related to the scheme $f_m + f_m \rightarrow 2\, f_m$. The biphase at this peak $\beta(f_m, f_m) = -42°$, and the phase shift of the second

harmonic $\Delta\phi_2$=42°. In a similar way, the bicoherence peak at $f \approx 4.8$ Hz with $b^2 = 0.30\text{-}0.35$ can be related to $f_m + 2f_m \rightarrow 3\ f_m$, and the phase shift of the third harmonic $\Delta\phi_3$=83°. Finally, the bicoherence peak at $f = 7.2$ Hz with $b^2 = 0.20\text{-}0.24$ can be related to $f_m + 3f_m \rightarrow 4\ f_m$, and the phase shift of the fourth harmonic $\Delta\phi_4$= 120°.

A relatively high bicoherence (and a stable non-random biphase) is observed not only at the bicoherence peaks but over all the frequency range $f > f_m$ as well (Fig.2c,d). While this "background" bicoherence $b^2 \approx 0.10\text{-}0.15$ is much lower than that at the peaks, it is still well above the 95% significance level $b_o^2 = 0.03$. Consequently, a noticeable phase coupling occurs between the dominant component f_m and all other spectral components.

A procedure described above was applied to all bispectral data. In most cases, the bicoherence at the major peak in the bicoherence spectrum at $f \approx f_m$ corresponding to the second harmonic was found to be from 0.4 to 0.6; from Eq. (3.1), the standard error for biphase (and, consequently, for $\Delta\phi_2$) is 3°-5°. The estimated phase shift of the second harmonic $\Delta\phi_2$ (Fig.3) increases consistently with the ratio u_*/C_m. The linear fit curve shown in Fig.3 is

$$\Delta\phi_2 = -5.1 + 33.5 \cdot (u_*/C_m) \qquad (4.2)$$

The observed variation of the phase shift $\Delta\phi_2$ with u_*/C_m is similar to that of the asymmetry data (Fig.1c). A strong correlation between $\Delta\phi_2$ and A is confirmed by the regression plot shown in Fig.4: the smallest phase shift corresponds to waves with zero asymmetry and the largest phase shift is observed for most asymmetrical waves with $A \approx -0.4$.

Now consider bispectral data for the third and fourth harmonic. In most cases, the bicoherence observed at the peaks $f \approx 2f_m$ and $f \approx 3f_m$ (see Fig.2c) was found to be 0.2-0.3, i.e., much lower than that at the major peak $f \approx f_m$. To increase statistical stability, the biphase data corresponding to the third and fourth harmonic were additionally averaged over 3x3 squares in (f_1, f_2) space and these averaged values were used to estimate the phase shifts $\Delta\phi_3$ and $\Delta\phi_4$ from Eq.(2.10). The standard error for $\Delta\phi_3$ and $\Delta\phi_4$ was estimated as 5°-15° and 10°-20°, respectively.

Variation of the phase shifts $\Delta\phi_3$ and $\Delta\phi_4$ with the ratio u_*/C_m is shown in Fig.5a,b. Despite scatter of the data, a consistent increase in both $\Delta\phi_3$ and $\Delta\phi_4$ with u_*/C_m is observed. The fit curves shown in Fig.5a,b are

$$\Delta\phi_3 = 14.3 + 52.9 \cdot (u_*/C_m) \qquad (4.3)$$

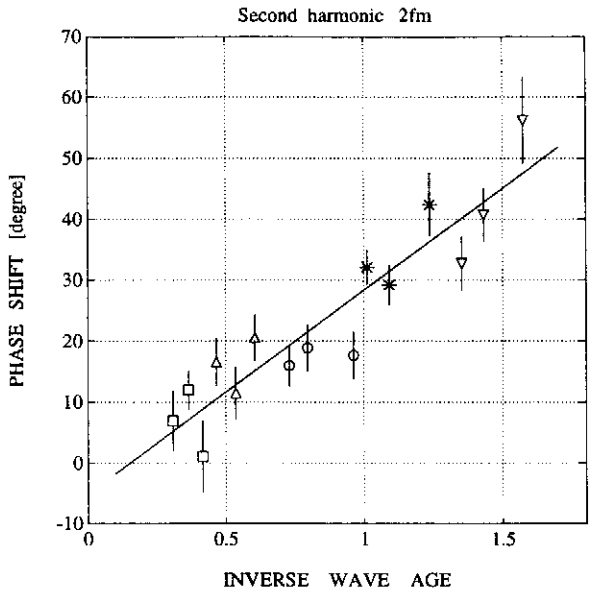

Fig.3. Variation of the phase shift of the second harmonic $\Delta\phi_2$ with inverse wave age u_*/C_m (for legend see Fig.1). Vertical bars are the standard errors; a solid line is the fit curve (4.2).

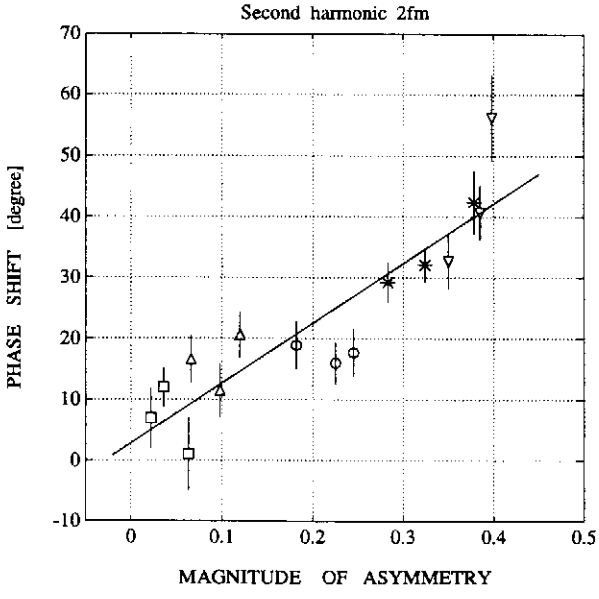

Fig.4. Correlation between the phase shift of the second harmonic $\Delta\phi_2$ and the magnitude of asymmetry -A. A solid line is the fit curve $\Delta\phi_2 = 2.8 + 98.2 \cdot (-A)$. For legend see Fig.1.

$$\Delta\phi_4 = 32.5 + 71.1 \cdot (u_*/C_m) \qquad (4.4)$$

In Fig.6 the phase shifts of harmonics are shown in a normalized form $\Delta\phi_2/2$, $\Delta\phi_3/3$, and $\Delta\phi_4/4$ to represent a phase shift in units of the phase of the dominant component f_m and to compare evolution of phase shifts for different harmonics. While the individual values of $\Delta\phi_2$, $\Delta\phi_3$, and $\Delta\phi_4$ vary over a broad range, the difference between the normalized phase shifts is very stable and virtually independent of the ratio u_*/C_m.

5 Discussion and Conclusions

Our results demonstrate that: 1) the profile of wind waves is markedly asymmetric under all conditions studied; and 2) there is a characteristic relationship between distortion of the wave profile and the degree of wave development. While the skewness S describing the horizontal asymmetry of waves, varies only slightly with fetch and/or wind speed and reveals no particular dependence on the inverse wave age u_*/C_m, the magnitude of asymmetry A that describes vertical asymmetry of waves increases consistently with the ratio u_*/C_m. The strong correlation found between A and u_*/C_m suggests that the vertical asymmetry of waves is caused by direct wind forcing.

Unfortunately, no field data on the asymmetry A are presently available for direct comparison with our data. Longuet-Higgins (1982) re-analyzed the sea-surface slope data of Cox and Munk (1956) to study the relationship between the skewness of slopes λ_3 (which roughly corresponds to our definition of asymmetry A) and the wind stress. His results can be presented in the following form

$$\lambda_3 = - cV^{3/2} \qquad (5.1)$$

(where c is an empirical coefficient, V is the wind speed) that shows both a negative sign for λ_3 and the increase of its magnitude with the wind speed. Consequently, the Eq.(5.1) is in qualitative agreement with our relationship (4.1); yet note that Cox and Munk's data, derived from sun glitter, represent slopes of all spectral components of the wave spectrum (including short gravity-capillary waves) and are likely to describe the asymmetry of short waves rather than that of the dominant waves.

Bailey et al. (1991) who used "an individual wave" concept found that the asymmetry of ocean waves is much lower than that in laboratory experiments. This conclusion is in agreement with more general evidence that mean (i.e., averaged over a long wave record)

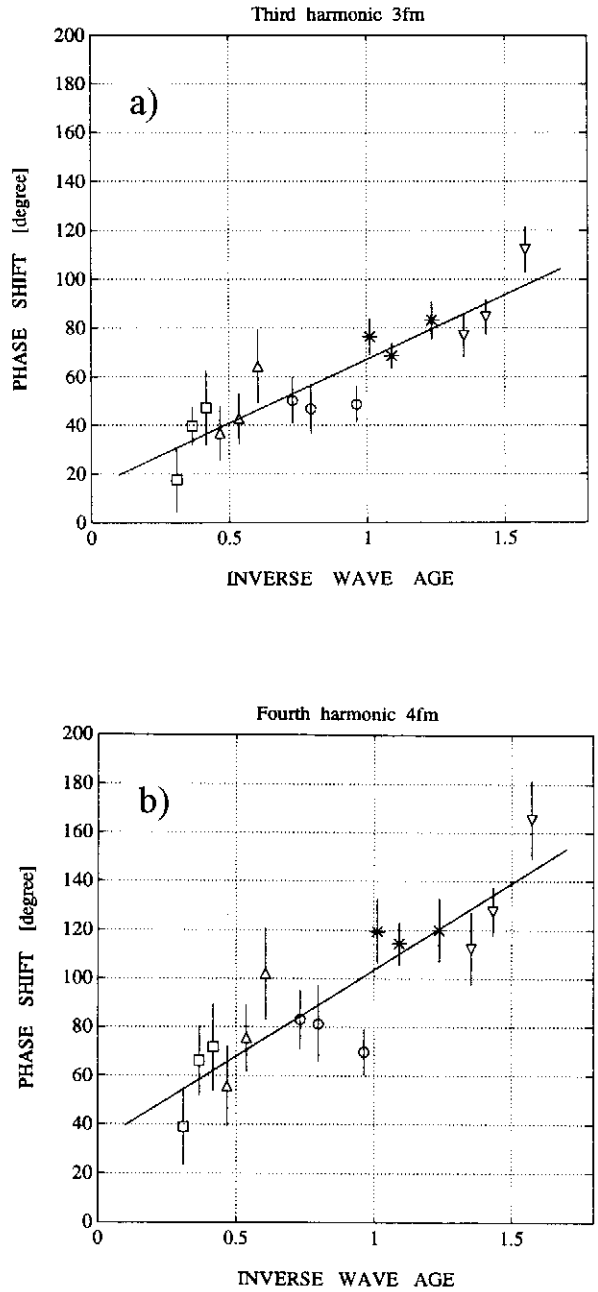

Fig.5. Dependence of the phase shifts of the third harmonic $\Delta\phi_3$ (a) and the fourth harmonic $\Delta\phi_4$ (b) on the inverse wave age u_*/C_m (for legend see Fig.1). Solid lines are the fit curves (4.3-4.4). Vertical bars are the standard errors.

nonlinear properties of dominant ocean waves are much less pronounced than that of laboratory waves (e.g., Leykin et al., 1984). However, due to the group structure of the wave field that is commonly observed in the ocean, some of the highest waves can be much steeper (i.e., more nonlinear) than would follow from mean estimates.

Consequently, comprehensive field observations of

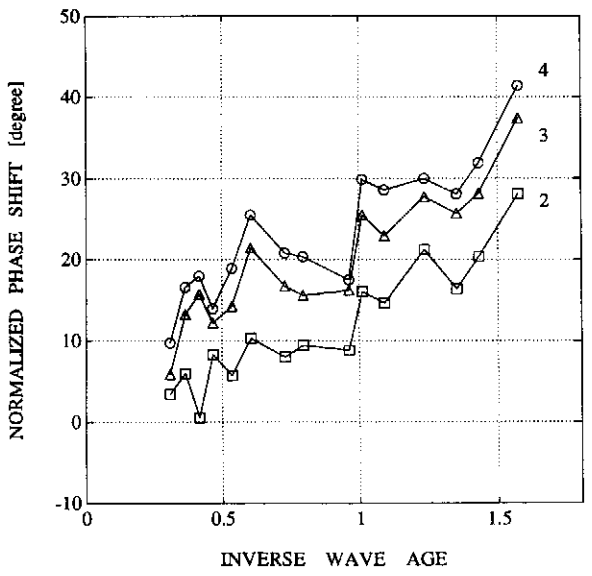

Fig.6. Evolution of the normalized phase shift of the first three harmonics with inverse wave age u_*/C_m. 2 - $\Delta\phi_2/2$ (the second harmonic); 3 - $\Delta\phi_3/3$ (the third harmonic); and 4 - $\Delta\phi_4/4$ (the fourth harmonic).

asymmetry of waves are desirable, and we believe that the nonlinear nonspectral concept combined with bispectral analysis provides a fruitful approach to this problem. Our results support the major assumption of this concept that the laboratory wind-wave field can be represented as a coherent system consisting mainly of the dominant component ω_m and its harmonics. We found that within relatively narrow bands located at the harmonically related frequencies $2\omega_m$, $3\omega_m$, and $4\omega_m$, bound components dominate or, at least, contribute substantially to the wave energy. This conclusion is in a good agreement with data of Donelan et al. (1985) who showed that the energy in the bound harmonics at $2\omega_m$ exceeds that in the free waves at the same frequency when $u_*/C_m > 0.3$.

Apparently, free (linear) components are also present in the wave spectrum. To some extent, nonlinear coupling is observed between ω_m and all other spectral components $\omega > \omega_m$ as well, but the contribution from this "background" coupling into the wave energy outside of the above mentioned bands is small. Nevertheless, as far as the waves' asymmetry is concerned, the nonlinear nonspectral concept describes wind waves satisfactorily enough because only bound components account for nonlinear distortion of the wave form and the resulting non-Gaussianity of the surface statistics.

An important addition to the nonlinear nonspectral concept that was found in our study is a phase shift between ω_m and its harmonics that increases consistently with the inverse wave age u_*/C_m. This result is in agreement with both common visual observations of wind waves and our present data on asymmetry A.

One can suggest that an advanced model based on the nonlinear nonspectral concept and accounting for the mentioned phase shift of harmonics can be used not only to describe waves with the asymmetric profile but to simulate such waves as well. For this purpose, the wave field can be represented as follows

$$\zeta(x, t) = a_m [\, \mathrm{Cos}(k_m x - \omega_m t) + a_2 \mathrm{Cos}(2 k_m x - 2\omega_m t + \Delta\phi_2) + a_3 \mathrm{Cos}(3k_m x - 3\omega_m t + \Delta\phi_3) + \ldots] \qquad (5.2)$$

where $a_m = \sqrt{2}\cdot\sigma$ is the r.m.s. magnitude of the dominant waves. The phase shifts $\Delta\phi_i$ and their dependence on the inverse wave age can be determined from our empirical relationships (4.2-4.4) shown in Fig.3, 5.

The model (5.2) is a semi-empirical description of the wave field rather than its rigorous physical representation (see Lake and Yuen, 1978). According to (5.2), a random wave field is replaced with a deterministic wave system with parameters that reflect some average properties of actual waves. Consequently, this is essentially a "local" representation that is valid only as far as averaged parameters of waves (e.g., ω_m and a_m) are not changing significantly with the wind speed and/or fetch.

In conclusion we note that properties of the relative magnitudes of harmonics a_i that are required for modeling but were not studied in the present work, will be condidered in a separate paper (Leykin et al., 1995) along with detailed descriptions of the proposed model and an analysis of its accuracy and limitations.

Acknowledgments. This work was supported by the Office of Naval Research under Contracts N00014-91-J-1782 (IAL and RHM), N000-1493-106-10 (IAL and DJM), and N000-1488-J-1028 (MAD). We are grateful to Victor I. Shrira for useful comments on the manuscript

References

Bailey, R.J., Jones, I.S.F., and Toba, Y., The steepness and shape of wind waves, *J. Oceanogr. Soc. Japan, 47*, 249-264, 1991

Cox, C.S., and Munk, W., Slopes of the sea surface deduced from photographs of sun glitter, *Bull. Scripps Inst. Oceanogr., 6*, 401-488, 1956.

Donelan, M.A., Hamilton, J., and Hui, W.H., Directional spectra of wind-generated waves, *Phil. Trans. R. Soc. Lond. A-315*, 509-562, 1985.

Elgar, S., Relationships involving third moments and bispectra of a harmonic process, *IEEE Trans. on Acoust. Speech and Signal Proc, ASSP-35*, 1725-1726, 1987.

Elgar, S., and Guza, R.T., Observations of bispectra of shoaling surface gravity waves, *J.Fluid Mech., 161*, 425-448, 1985.

Elgar, S., and Sebert, G., Statistics of bicoherence and biphase, *J.Geophys.Res., 94*, 10,993-10,998, 1989.

Goncharov, V.V., and Leykin, I.A., Waves in a current with velocity shear, *Oceanology, 23*, 155-159, 1983.

Hasselmann, K., Munk, W., and MacDonald,G., Bispectra of ocean waves, In: *Time series analysis* (Ed. M. Rosenblatt), pp. 125-139, Wiley, 1963.

Haubrich, R.A., Earth noises, 5 to 500 millicycles per second, *J.Geophys.Res., 70*, 1415-1427, 1965.

Huang, N.E., and Long, S.R., An experimental study of the surface elevation probability distribution and statistics of wind-generated waves, *J.Fluid.Mech., 101*, 179-200, 1980.

Imasato, N., and Kunishi,H., Bispectra of wind waves and wave-wave interaction, *J. Oceanogr. Soc. Japan, 33*, 267-271, 1977.

Kim, I.C., and Powers, E.J., Digital bispectral analysis and its applications to nonlinear wave interactions, *IEEE Trans. Plasma Science, 1*, 120-131, 1979.

Lake, B.M., and Yuen, N.C., A new model for nonlinear wind waves. Pt.1. Physical model and experimental evidence, *J.Fluid.Mech., 88*, 33- 62, 1978.

Leykin, I.A., and McLaughlin, D.J., Modeling the asymmetric wave form of wind waves based on bispectral analysis of wave records, Submitted to: *J.Geophys.Res.*, 1995.

Leykin, I.A., Pokazeyev, K.V., and Rozenberg, A.D., Growth and equilibrium of the wind waves in a laboratory channel, *Izv. Atmos. Oceanic Phys., 20*, 313-318, 1984.

Longuet-Higgins, M.S., On the skewness of sea-surface slopes, *J. of Phys. Oceanogr., 12*, 1283-1291, 1982.

Masuda, A., and Kuo, Y.Y., A note on the imaginary part of bispectra, *Deep-Sea Res., 28*, 213-222, 1981.

McComas, C.H., and Briscoe, M.G., Bispectra of internal waves, *J.Fluid Mech., 97*, 205-213, 1980.

Nikias, C.N., and Raghuveer, M.R., Bispectral estimation: a digital signal processing framework, *Proc. IEEE, 75*, 869-891, 1987.

Ocampo-Torres, F.J., Donelan, M.A., Mergi, N., and Jia, F., Laboratory measurements of mass transport of carbon dioxide and water vapor for smooth and rough flow conditions, *Tellus, 46B*, 16-32, 1994.

Ocampo-Torres, F.J., Donelan, M.A., and Piroth, K. Drift velocity profiles, (In preparation), 1995.

Phillips, O.M., *The dynamics of the upper ocean* (2nd edn), 336 p. Cambridge University Press, 1977.

Plate, E.J., The role of the dominant wave in the spectrum of wind-generated water surface waves, In: *Proc. 9th Symposium on Naval Hydrodynamics, v.2*, pp.1371-1396, Paris, 1972.

Ramamonjiarisoa, A., and Coantic, M., Loi expérimentale de dispersion des vagues produites par le vent sur une faible longeur d'action, *Comptes Rendus Acad. Sc, Paris, 283 B*, 111-114, 1976.

Shrira, V.I., Surface waves on shear currents: solution of the boundary- value problem, *J.Fluid Mech., 252*, 565-584, 1993.

Stewart, R.H., and Joy, J.W., HF radar measurements of surface currents, *Deep-Sea Res., 21*, 1039-1049, 1974.

Wu, J., Wind-induced drift currents, *J.Fluid Mech., 68*, 49-70, 1975.

Yefimov, V.V., and Kalmykov, V.A., Dependence of wind-wave bispectra on the sea state, *Oceanology, 24*, 598-604, 1984.